

Peculiar Magnetism of the $\text{Sm}_{(1-x)}\text{Gd}_x\text{TiO}_3$ System

G. Amow, J.-S. Zhou, and J. B. Goodenough¹

Texas Materials Institute, C2201, University of Texas, Austin, Texas, 78712

Received May 30, 2000; in revised form July 5, 2000; accepted July 28, 2000; published online September 30, 2000

Magnetic susceptibility measurements were made on polycrystalline samples of the system $\text{Sm}_{(1-x)}\text{Gd}_x\text{TiO}_3$ ($0.10 \leq x \leq 1.0$) and on single-crystal GdTiO_3 . A systematic decrease in the magnetic ordering temperature with increasing $x < 0.5$, falling below 5 K at $x = 0.5$ and increasing with $x > 0.5$, was interpreted to signal a competition between antiferromagnetic and ferromagnetic coupling among itinerant π^* electrons of the TiO_3 array. In a field $H > 1$ kOe, GdTiO_3 approached saturation with a moment of $6 \mu_B$ /formula unit, consistent with collinear-spin ferrimagnetism. Semicovalent exchange was invoked to justify the observed antiferromagnetic coupling between Gd(III) and Ti(III) spins. However, the M - H curves taken in ± 50 kOe were unusual; they were essentially anhysteretic with no measurable remanence or coercivity, but a small ferromagnetic component observed in 20 Oe was typical of a weak, canted-spin ferromagnetism on an antiferromagnetic TiO_3 array. The lack of hysteresis and the approach to a ferrimagnetic saturation in high magnetic fields was found for all x for small as well as high applied fields. Although the TiO_3 array orders antiferromagnetically below a critical temperature, a ferromagnetic moment was induced on the TiO_3 array by an applied magnetic field and by the molecular field associated with antiferromagnetic Gd-Ti interactions. The applied H required to saturate the ferromagnetic moment on the TiO_3 array decreased with increasing x . © 2000 Academic Press

Key Words: magnetic order; magnetic exchange; exchange inversion; itinerant-electron magnetism.

INTRODUCTION

The structural and physical properties of the octahedrally distorted ($Pnma$) titanates RTiO_3 ($R = \text{La-Lu, Y, and mixtures thereof}$) exhibit unusual physical properties (1–8). The single d electron of the octahedral Ti(III) site occupies a narrow π^* band. All the oxygen stoichiometric titanates are magnetic insulators; the bandwidth is on the narrow side of the Mott-Hubbard transition. The energy gap between the Ti(IV)/Ti(III) and Ti(III)/Ti(II) redox bands increases

from 0.01 to 0.22 eV on going from La to Y [1], which is consistent with a narrowing of the π^* band as the size and basicity of the R (III) ion decreases (9). However, there is no evidence of a cooperative Jahn-Teller orbital ordering or of an important contribution to the magnetic moment and crystalline anisotropy from a localized-electron orbital angular momentum of the TiO_3 array in any of the titanates from antiferromagnetic LaTiO_3 to ferromagnetic YTiO_3 and LuTiO_3 . They all appear to exhibit itinerant-electron magnetism on the TiO_3 array. Therefore, it is worth noting that antiferromagnetic LaTiO_3 (type G order) exhibits a weak, canted-spin ferromagnetic moment due to an anti-symmetric exchange with a Dzyaloshinsky vector, \mathbf{D} , parallel to the a axis in $Pnma$ (b axis in $Pbnm$) of the orthorhombic unit cell.

Of particular interest for this study is a transition from antiferromagnetic to ferromagnetic coupling in the TiO_3 array as x increases in the system $\text{La}_{(1-x)}\text{Y}_x\text{TiO}_3$ (3, 5). Since the atomic orbitals contributing to the π^* bands are less than one-quarter filled, a ferromagnetic order is predicted unless the width W_π of the π^* is too broad for the intraatomic exchange interaction to raise the occupied states of the minority-spin band completely above the Fermi energy. A transition from band antiferromagnetism to band ferromagnetism has been anticipated for decreasing width of a band derived from degenerate orbitals that is less than one-quarter filled (9). On the other hand, the $\text{La}_{(1-x)}\text{Y}_x\text{TiO}_3$ system represents the only known experimentally demonstrated example of such a transition occurring in the absence of coexisting localized atomic moments. However, this fact was not recognized because the observed decrease with increasing x of the antiferromagnetic Néel temperature, T_N , was assumed to signal the presence of localized d^1 configurations in the antiferromagnetic compositions (10). Indeed, for a band derived from half-filled orbitals as in LaCrO_3 or LaFeO_3 , T_N increases unambiguously with the strength of the superexchange interactions between localized-electron spins on neighboring atoms, but decreases with increasing bandwidth for itinerant-electron antiferromagnetism. However, this prediction does not apply where the band is derived from degenerate orbitals that are less than

¹To whom correspondence should be addressed. Fax: (512) 471-7681. E-mail: jbgoodenough@mail.utexas.edu.



one-quarter filled. The system $\text{La}_{(1-x)}\text{Y}_x\text{TiO}_3$ demonstrates that, in this case, the T_N for band antiferromagnetism decreases with narrowing bandwidth to near zero at the crossover from antiferromagnetic to ferromagnetic order. On the other hand, the ferromagnetic Curie temperature, T_C , increases with decreasing bandwidth as expected for band ferromagnetism.

Previous experiments (3) have suggested that a similar transition on the TiO_3 array occurs in the presence of rare-earth localized atomic moments in the system $\text{Sm}_{(1-x)}\text{Gd}_x\text{TiO}_3$. In this paper, we demonstrate a systematic lowering of T_N with $x < 0.5$ and raising of the magnetic-ordering temperature with $x > 0.5$ in this system; long-range magnetic order disappears above 5 K at the crossover composition $x = 0.5$. We also report a study of a single crystal of GdTiO_3 that explores the evolution of magnetic order with the strength of an applied magnetic field. We compare the effect on the magnetic-ordering temperature of increasing the bandwidth W_π of GdTiO_3 by applying hydrostatic pressure and by substituting Sm.

EXPERIMENTAL PROCEDURES

The members of the solid solution system $\text{Sm}_{(1-x)}\text{Gd}_x\text{TiO}_3$ ($0.10 \leq x \leq 1.00$, $\Delta x = 0.10$) investigated in this study were prepared by conventional solid-state methods. Stoichiometric amounts of Gd_2O_3 (Alfa, 99.99%), Sm_2O_3 (Alfa, 99.99%), and Ti_2O_3 (Cerac, 99.99%) were mixed intimately in acetone in a ball mill for approximately 12 h. The rare-earth oxides were calcined at 1000°C for at least 12 h to remove any carbonates or hydroxides prior to weighing. For each composition, the powder was made into 1-in. pellets, placed into an open molybdenum crucible, and fired in a vacuum furnace ($\sim 10^{-5}$ Torr) for 10–12 h at 1400°C .

A single crystal of GdTiO_3 was grown by the floating-zone method in an NEC SC-M35HD double-ellipsoid image furnace. Polycrystalline GdTiO_3 prepared as described above was made into seed and feed rods that were subsequently sintered in the vacuum furnace at 1200°C for 10 h. The single crystal was grown in a flowing 10% H_2 -Ar gas mixture (3.0 L/min flow rate). The size of the crystal obtained was ~ 1 cm in length \times 4 mm in diameter; it was subsequently oriented along the major axes by means of Laue photography.

Phase purity determinations for all compositions were performed with X-ray powder diffraction and $\text{CuK}\alpha$ radiation in a Philips Norelco step scanning diffractometer. For the determination of the unit-cell constants, data were collected with a silicon standard in 0.02° steps over a two-theta range of 10° – 80° with a count time of 10 s per step. The refinement of the unit-cell constants was performed with a least-squares method in the program JADE.

The oxygen content for each composition was determined by thermogravimetric analysis with a Perkin-Elmer TGA7

system from the weight gain observed when oxidized in flowing air at 1000°C . The oxygen content per formula unit was determined to be 3.02 ± 0.02 based on the nominal content of rare-earth and transition-metal atoms with the exception of the $x = 0.30$ and 0.40 compositions, which were slightly more oxidized with values of 3.04 ± 0.02 .

Direct current susceptibility and magnetization measurements were carried out with a SQUID magnetometer (Quantum Design MPMS). Typical sample sizes were ~ 20 – 30 mg with an applied field of 2.5 kOe. Measurements were performed on heating after cooling in zero field (ZFC) and the measuring field (FC). In addition, complete hysteresis loops were obtained at 5 K in a magnetic field range of ± 50 kOe.

High-pressure ac magnetic-susceptibility measurements were made with a home-built apparatus (J.-S. Zhou, unpublished). Data were taken under several applied pressures ranging from 1 bar to ~ 22 kbar with an applied field of 10 Oe.

RESULTS

I. Structure. The X-ray powder pattern for GdTiO_3 (Fig. 1) is typical of those found for all compositions of the $\text{Sm}_{(1-x)}\text{Gd}_x\text{TiO}_3$ system. All the peaks could be indexed with a perovskite structure of orthorhombic GdFeO_3 in the standard $Pnma$ setting; no impurity phase could be detected. The unit-cell constants obtained by a least-squares refinement with a silicon standard are shown in Fig. 2 and tabulated in Table 1. The cell parameters for polycrystalline GdTiO_3 are in good agreement with those previously reported: $a = 5.393$ Å, $b = 5.691$ Å, and $c = 7.664$ Å (2). The data reveal a systematic decrease in the unit-cell parameters and volume with increasing content, x , of the smaller Gd(III) ion.

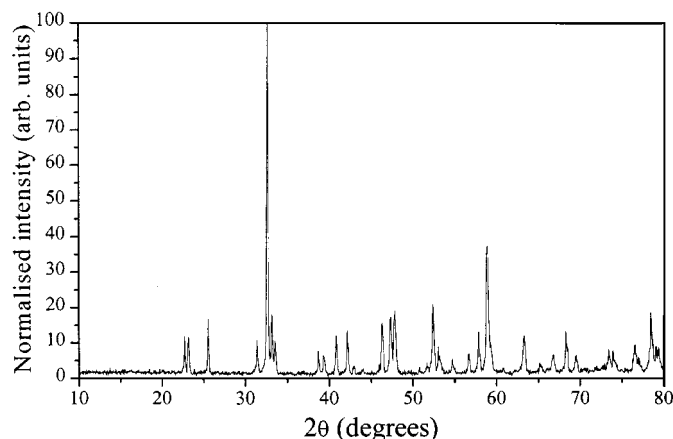


FIG. 1. X-ray powder diffraction pattern for GdTiO_3 at room temperature.

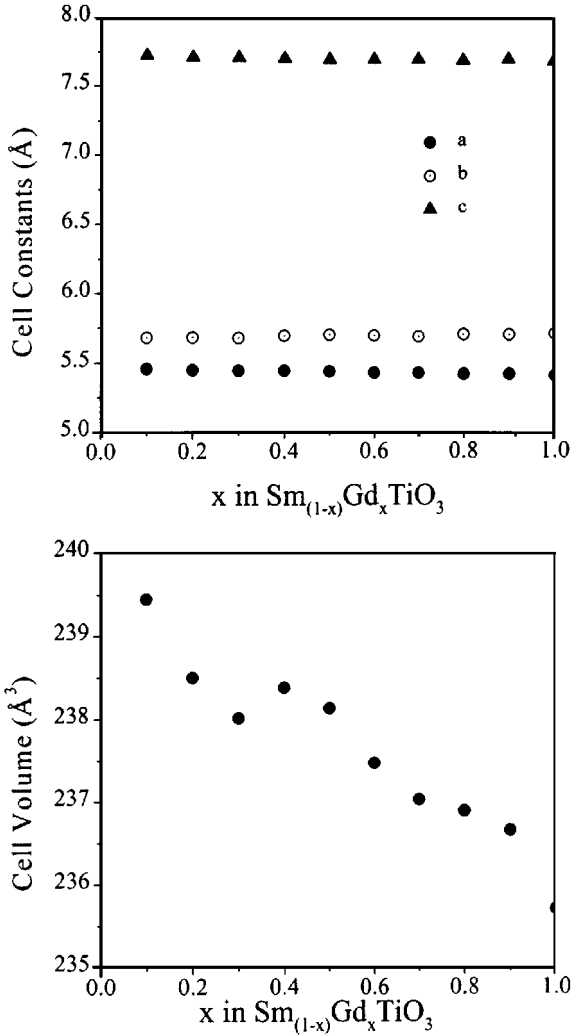


FIG. 2. Unit-cell constants vs x in $\text{Sm}_{(1-x)}\text{Gd}_x\text{TiO}_3$.

II. Magnetic data. Figure 3a shows the dc susceptibility taken on single-crystal GdTiO_3 along the three major axes in a field of 2.5 kOe. In this field, the χ^{-1} versus T curves of Fig. 3b are typical of ferrimagnetic behavior with a Weiss constant $\theta \approx -25$ K, a Curie temperature $T_C \approx 29(1)$ K, and little magnetocrystalline anisotropy in the paramagnetic phase. The T_C is reduced from the value of 32(1) K obtained for the polycrystalline sample; it appears that a slight oxidation occurred during crystal growth.

Moreover, the M - H curves for single-crystal GdTiO_3 taken at 5 K along the three major crystallographic axes (Fig. 4) show a saturation moment of $6 \mu_B$ /formula unit in agreement with a previously reported polycrystalline value. Based on this saturation moment, a spin-only ferrimagnetic order has been proposed in which the $\text{Gd(III)}:4f^7$ and $\text{Ti(III)}:3d^1$ spins are coupled antiferromagnetically to one another. However, although this collinear ferrimagnetic model appears to apply in a saturation magnetic field, it

TABLE 1
Unit-Cell Constants of $\text{Sm}_{(1-x)}\text{Gd}_x\text{TiO}_3$ System ($0.00 \leq x \leq 1.00$) from Least-Squares Refined Data with Silicon Standard

Compound	a (Å)	b (Å)	c (Å)	$V/(\text{Å}^3)$
GdTiO_3	5.3954(16)	5.6955(18)	7.6642(22)	235.52(21)
$\text{Gd}_{0.90}\text{Sm}_{0.10}\text{TiO}_3$	5.4109(7)	5.6911(10)	7.6849(12)	236.65(11)
$\text{Gd}_{0.80}\text{Sm}_{0.20}\text{TiO}_3$	5.4124(9)	5.6959(11)	7.6838(14)	236.88(13)
$\text{Gd}_{0.70}\text{Sm}_{0.30}\text{TiO}_3$	5.4216(10)	5.6808(11)	7.6959(14)	237.02(13)
$\text{Gd}_{0.60}\text{Sm}_{0.40}\text{TiO}_3$	5.4231(10)	5.6880(9)	7.6982(12)	237.46(12)
$\text{Gd}_{0.50}\text{Sm}_{0.50}\text{TiO}_3$	5.4325(50)	5.6947(29)	7.6975(9)	238.13(36)
$\text{Gd}_{0.40}\text{Sm}_{0.60}\text{TiO}_3$	5.4392(21)	5.6855(20)	7.7055(26)	238.29(22)
$\text{Gd}_{0.40}\text{Sm}_{0.60}\text{TiO}_3$	5.4329(12)	5.6848(13)	7.7084(15)	238.07(15)
$\text{Gd}_{0.30}\text{Sm}_{0.70}\text{TiO}_3$	5.4395(19)	5.6741(21)	7.7114(25)	238.01(25)
$\text{Gd}_{0.20}\text{Sm}_{0.80}\text{TiO}_3$	5.4459(13)	5.6786(14)	7.7122(16)	238.50(17)
$\text{Gd}_{0.10}\text{Sm}_{0.90}\text{TiO}_3$	5.4578(41)	5.6795(24)	7.7248(7)	239.45(30)

cannot account for the lack of any hysteresis in the M - H curves, which have zero remanence and coercivity.

To investigate this unusual magnetic behavior, the field dependence of the magnetic susceptibility was studied. The

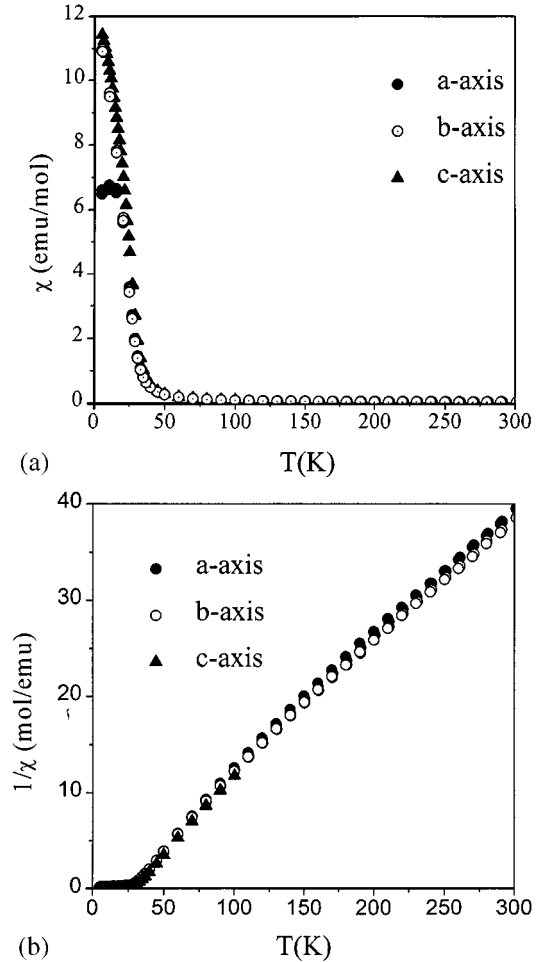


FIG. 3. (a) χ vs T and (b) $1/\chi$ vs T for GdTiO_3 at 2.5 kOe.

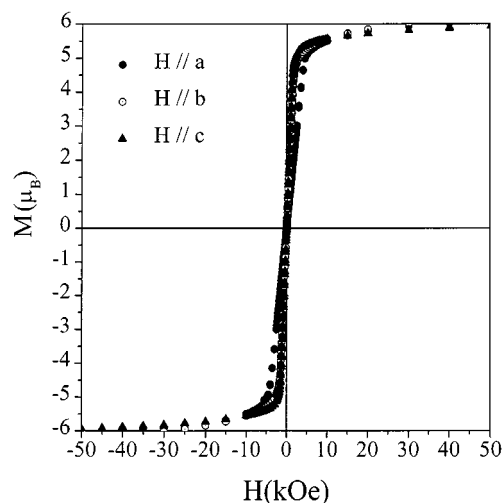


FIG. 4. Magnetization versus applied field for single-crystal GdTiO_3 .

Weiss constant, $\theta \approx -25$ K, is independent of the applied field. Figure 5 shows a divergence in the measuring field of 20 Oe between the curves taken after ZFC and FC. A similar behavior was found for the antiferromagnetic compounds NdTiO_3 and SmTiO_3 , both of which exhibit a weak, canted-spin ferromagnetism (8, 11). However, at higher fields the divergence of Fig. 5 disappears. With both low and high maximum fields, the M - H curves were without hysteresis within the experimental error of our SQUID magnetometer. Where M reaches saturation, the $\chi = M/H$ curves of Fig. 6 decrease with increasing H . The field at which saturation is achieved is strongly dependent on the crystal axis along which the field H is applied. The a axis is the direction of hard magnetization and the c axis is the easy

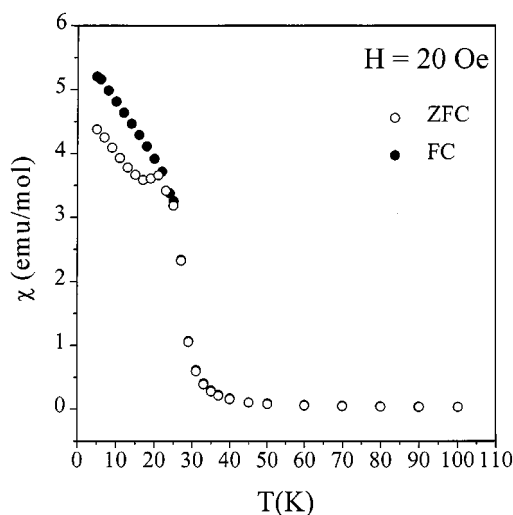


FIG. 5. χ vs T for single-crystal GdTiO_3 at low field showing divergence between ZFC and FC data.

magnetization direction, as is also evident in the M - H curves of Fig. 4. Figure 6 is representative of all compositions $x \geq 0.4$.

The high-pressure ac susceptibility of single-crystal GdTiO_3 is shown in Fig. 7. A small, systematic decrease in the magnetic-ordering temperature occurs with increasing applied pressure from 1 bar to 20 kbar; it falls by 1 K in this pressure range.

Figure 8 shows the dc susceptibility taken at 2.5 kOe for the polycrystalline samples of the system $\text{Sm}_{(1-x)}\text{Gd}_x\text{TiO}_3$; the M versus H curves taken at 5 K are shown in Fig. 9. Antiferromagnetic SmTiO_3 displays a weak, canted-spin ferromagnetism in an applied field H . Nevertheless, as in the case of GdTiO_3 , all the M - H curves taken over the range ± 50 kOe exhibit no apparent hysteresis; the saturation moment increases monotonically with the Gd concentration, x , and the saturation field decreases. On the other hand, the long-range magnetic-ordering temperature decreases systematically with $x < 0.5$, falling below 5 K at $x = 0.5$, but increases with x in the range $0.5 < x < 1.0$ (see Fig. 10). Comparison with the $\text{La}_{(1-x)}\text{Y}_x\text{TiO}_3$ system would suggest that a crossover from predominantly antiferromagnetic to predominantly ferromagnetic interactions within the TiO_3 array occurs near $x = 0.5$.

DISCUSSION

The GdTiO_3 saturation magnetization of $6 \mu_B$ /formula unit clearly shows the existence of an antiferromagnetic 90° Gd-O-Ti superexchange interaction. The Gd(III): $4f^7$ energy level lies below the top of the O: $2p^6$ valence bands, so the dominant virtual charge transfer in the superexchange interaction is from the TiO_3 array to the empty Gd- $5d$ band having its spin parallel to the localized spin $S = \frac{7}{2}$ of the Gd(III): $4f^7$ configuration. Conservation of spin angular momentum during charge transfer would dictate a ferromagnetic interaction if transfer of a π^* electron were preferred. Therefore, we must consider an alternate superexchange interaction. We note that the Gd- $5d$ band σ -bonds with the O- $2p$ orbitals that π -bond with the Ti(III) ions. The Gd: $5d$ -O: $2p$ covalent bonding stabilizes the O- $2p$ spin state that is parallel to the Gd spin, which leaves the O- $2p$ spin state that is antiparallel to the Gd spin to π -bond more strongly with the Ti(III) ions. This example of semicovalent superexchange postulated years ago (12) is interesting because, in this case, it has a spin opposite to that of a conventional superexchange and is dominant. For 180° M-O-M interactions, the two contributions have the same sign so that it is not possible to distinguish experimentally their relative magnitudes. Semicovalent exchange is normally smaller than conventional superexchange as it involves a two-electron transfer from the oxygen atom. However, in GdTiO_3 it is particularly strong because of the large intraatomic exchange coupling between a $5d$ electron spin and

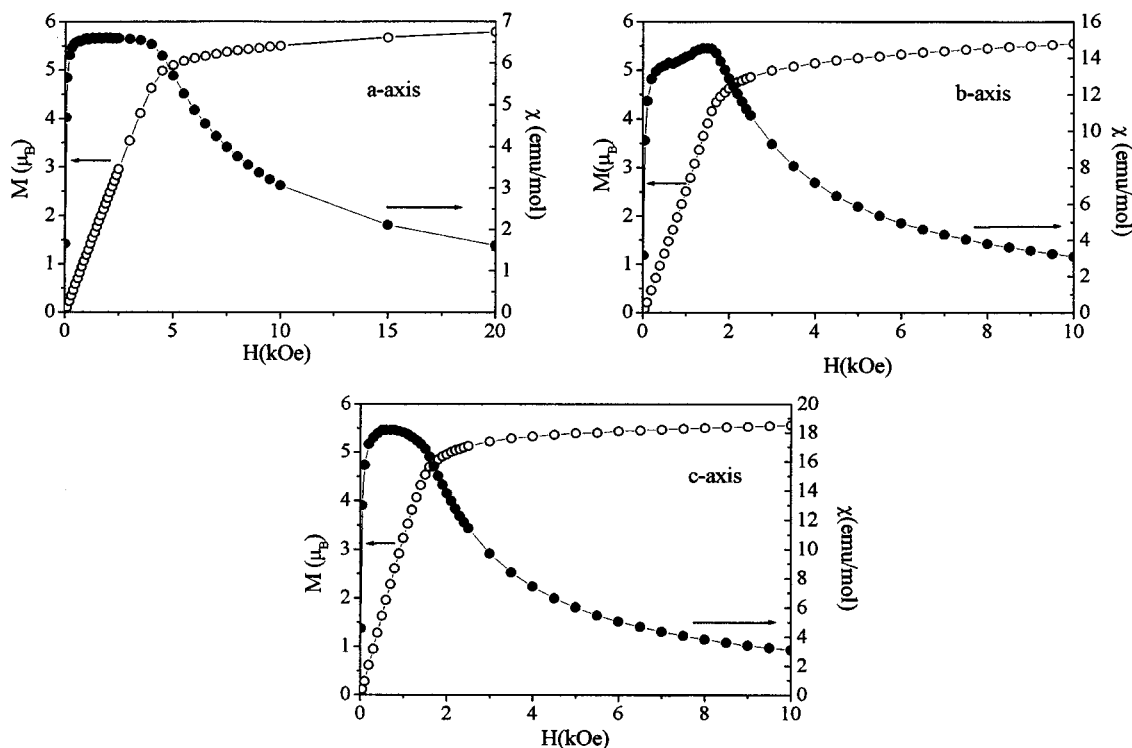


FIG. 6. χ vs H and M vs H curves for single-crystal GdTiO_3 at 5 K.

the localized spin $S = \frac{7}{2}$ of the $\text{Gd(III)}:4f^7$ configuration; also the large overlap of the Gd-5d and O-2p orbitals gives the Gd-O bond a significant covalent component.

Antiferromagnetic order in GdAlO_3 shows that the Gd-Gd interactions are antiferromagnetic (13), but they are very weak. The magnetic interactions between the π^* electrons of the TiO_3 array are dominant even though they

appear to be weakened by competition from antiferromagnetic to ferromagnetic interactions, particularly at $x \approx 0.5$ in $\text{Sm}_{(1-x)}\text{Gd}_x\text{TiO}_3$. In the titanates with heavier rare-earth ions (TbTiO_3 , DyTiO_3 , and HoTiO_3), the π^* electrons are ferromagnetically aligned and the rare-earth spins have

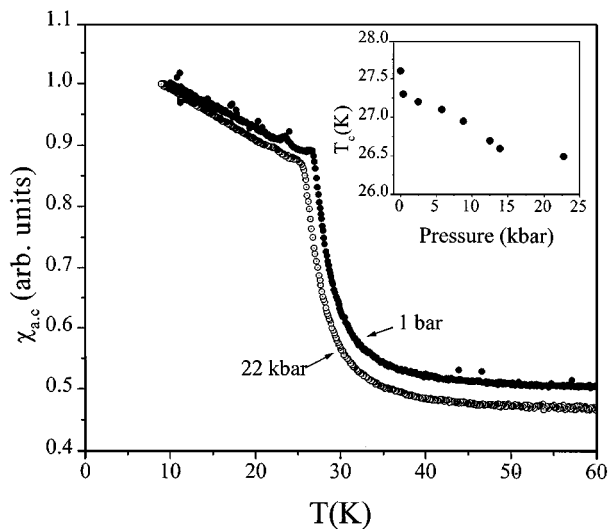


FIG. 7. χ_{ac} vs applied pressure for single-crystal GdTiO_3 along the c axis.

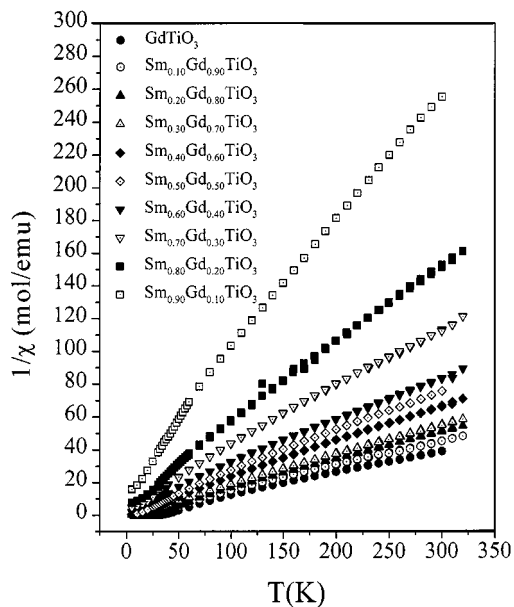


FIG. 8. $1/\chi$ vs T for $\text{Sm}_{(1-x)}\text{Gd}_x\text{TiO}_3$ system.

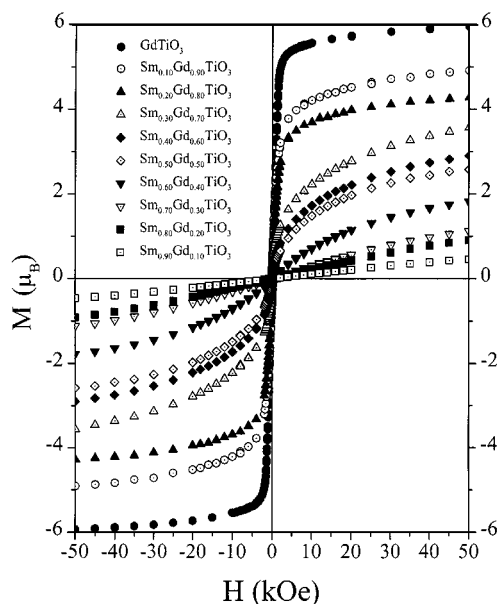


FIG. 9. Magnetization versus applied field for the $\text{Sm}_{(1-x)}\text{Gd}_x\text{TiO}_3$ system.

a canted C-type antiferromagnetic arrangement (C_yF_x or C_xF_y) (14, 15). In the transitional compound GdTiO_3 , the ferromagnetic interactions between π^* electrons are weaker, and the Ti(III) spins may be ordered antiferromagnetically where the antiferromagnetic interactions are competitive. Our problem is to understand how these competing interactions give rise to the observed magnetic behavior.

First, we note that there is no orbital angular momentum in the ground-state $4f^7$ configuration, and itinerant π^* electrons have an orbital angular momentum that is strongly reduced from that of a localized-electron configuration.

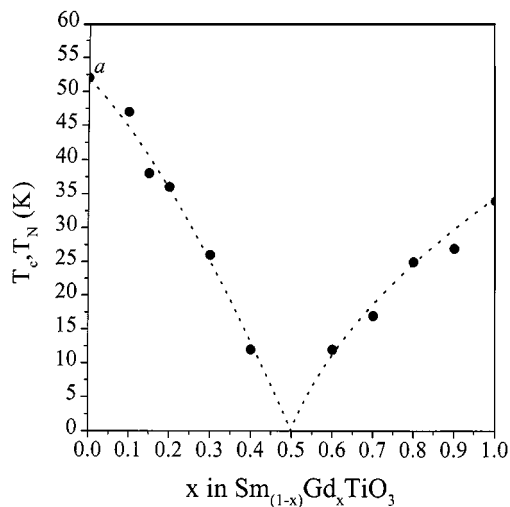


FIG. 10. T_C , T_N vs x in $\text{Sm}_{(1-x)}\text{Gd}_x\text{TiO}_3$. ^aFrom Ref. (8).

Consequently, the magnetocrystalline anisotropy is small, and the principal impediment to rotation of the spins in a magnetic field is the interatomic exchange field. In SmTiO_3 , the antiferromagnetic interactions among the π^* electrons are strong enough to resist a significant canting of the Ti(III) spins even in a field of 50 kOe. However, in GdTiO_3 the Gd spins are rotated from antiferromagnetic to ferromagnetic alignment in a field of 1 kOe at 5 K, and ferromagnetic alignment of the Gd spins appears to align the Ti(III) spins in an opposite direction. A hard a axis ($Pnma$) is consistent with a Dzyaloshinsky vector, \mathbf{D} , parallel to the a axis; antisymmetric exchange stabilizes the spins in the b - c plane.

Lack of a remanence in the M - H curves indicates an antiferromagnetic ground state in GdTiO_3 in zero applied field, but a weak, canted-spin ferromagnetic component is induced by a magnetic field, applied or molecular, on the TiO_3 array. The data in Fig. 9 show that at 5 K the Gd moments become aligned in the direction of the applied H field even in the $x = 0.5$ sample having no observable long-range magnetic order above 5 K in zero applied field. For a Gd concentration $x \geq 0.8$, saturation is approached in a polycrystalline sample by $H = 1$ kOe; ferromagnetic interactions in the TiO_3 array would favor an approach to ferrimagnetic saturation in a lower applied field. The available data do not provide information on the character of the antiferromagnetic order of GdTiO_3 in zero applied field. Both the Gd and the Ti subarrays of GdTiO_3 must be antiferromagnetically ordered, but the spins of each subarray are rotated smoothly in an H field to form a collinear-spin ferrimagnetic array in a field of only 1 kOe. The problem is to understand how this is possible.

With $x \leq 0.5$ in $\text{Sm}_{(1-x)}\text{Gd}_x\text{TiO}_3$, the Gd subarray appears to be paramagnetic at 5 K, but coupled antiferromagnetically to any canted-spin ferromagnetism of the TiO_3 array. As an applied H field increases, the Gd spins become more aligned, and the Gd-Ti interactions correspondingly increase the antiferromagnetically aligned canted-spin ferromagnetic moment of the TiO_3 array. A larger ferromagnetic moment on the TiO_3 array would feed back a larger molecular field to align the Gd spins.

For $x > 0.5$, the magnetic interaction on the TiO_3 array appears to change from predominantly antiferromagnetic to predominantly ferromagnetic, but the intraatomic exchange is not strong enough to remove fully the spin degeneracy of the π^* band at any value of x . In this case, we should expect either a progressive increase with T_C in the ferromagnetic component of the π^* electrons or the appearance of a spiral-spin configuration. Moreover, the Gd-Ti interactions increase in strength with the concentration of Gd(III) ions. Therefore, saturation of a collinear, ferrimagnetic spin configuration occurs in a lower applied H as x increases. The lack of any hysteresis in the M - H curves shows antiferromagnetic order at $H = 0$, which suggests that a

spin-density wave (SDW) is stabilized on the TiO_3 array. A SDW would weaken the Gd–Ti interactions to render the Gd array paramagnetic. However, alignment of the Gd spins in an applied H field induces a molecular field on the TiO_3 array that apparently stabilizes a ferromagnetic component on the TiO_3 array oriented antiparallel to the Gd magnetization, thereby increasing the Gd–Ti interactions and hence the Weiss molecular field at the TiO_3 array in a positive feedback. The greater the concentration of Gd(III) ions, the stronger the molecular field exerted by the Gd on the TiO_3 array; and for $x \geq 0.8$, a full ferrimagnetic moment is achieved at relatively low fields, $H \approx 1$ kOe.

CONCLUSIONS

The antibonding electrons of the TiO_3 array are not localized Ti(III): d^1 electrons; they occupy an itinerant electron π^* band on the strong-correlation side of the Mott–Hubbard transition. Therefore there is no cooperative Jahn–Teller deformation of the Ti(III) octahedral sites, and the orbital angular momentum of the itinerant π^* electrons is strongly suppressed.

Single-crystal GdTiO_3 has been shown to exhibit a saturation moment of $6 \mu_B$ /formula unit in large magnetic fields. We interpret this moment to signal a collinear-spin ferrimagnetism in fields $H > 1$ kOe. To justify an antiferromagnetic superexchange interaction between Gd(III) and Ti(III) spins, we were forced to conclude that semicovalent exchange associated with the O-2p electrons that σ -bond with the Gd and π -bond with the Ti dominates over virtual charge transfer of a π^* electron of the TiO_3 array to the empty Gd-5d band.

Magnetic-susceptibility measurement of single-crystal GdTiO_3 showed little anisotropy in the paramagnetic phase and identified, below the magnetic-ordering temperature, the orthorhombic a axis ($Pnma$) as a hard magnetization axis with little magnetocrystalline anisotropy in the b – c plane. In the absence of a significant orbital angular momentum on the Gd(III): $4f^7$ configuration or for the itinerant π^* electrons, a planar easy axis may be associated with an antisymmetric term with a Dzyaloshinsky vector along the a axis.

Although the magnetization M of GdTiO_3 saturates in a field of 1 kOe, the M – H curves show little hysteresis; there is almost no remanence or coercivity. However, the presence of a weak ferromagnetic moment was observed in low (~ 20 Oe) magnetic fields, which shows the presence of a weak canted-spin ferromagnetism as is found in the TiO_3 arrays of other $R\text{TiO}_3$ perovskites with an antiferromagnetic TiO_3 sublattice.

On the other hand, the $\text{Sm}_{(1-x)}\text{Gd}_x\text{TiO}_3$ system has been shown to exhibit a long-range magnetic-ordering temperature that decreases with increasing $x < 0.5$, falling below 5 K at $x = 0.5$, and increases with $x > 0.5$. Observation of

a change from antiferromagnetic order in the TiO_3 sublattice of the $R\text{TiO}_3$ family with $R = \text{La}$ to Sm to ferromagnetic order with $R = \text{Tb}$ – Lu places GdTiO_3 close to the transition between the two types of magnetic order on the TiO_3 array. By analogy with the $\text{La}_{(1-x)}\text{Y}_x\text{TiO}_3$ system, which shows a lowering (disappearance) of long-range magnetic order on the TiO_3 array in the transition region, we postulate that a transition from predominantly antiferromagnetic to predominantly ferromagnetic interactions among π^* electrons occurs near $x = 0.5$ in the $\text{Sm}_{(1-x)}\text{Gd}_x\text{TiO}_3$ system. An antiferromagnetic order on the TiO_3 array of GdTiO_3 in zero magnetic field indicates that the intraatomic exchange field remains too weak to remove completely the spin degeneracy of the π^* band, so a SDW is stabilized in zero applied field H . However, stabilization of ferromagnetic order on the TiO_3 array is accomplished by the Weiss molecular field associated with ordering of the Gd(III) spins in an applied magnetic field, and a positive feedback allows stabilization of a collinear-spin ferrimagnetism in only 1 kOe in GdTiO_3 .

Finally, the decrease in magnetic-ordering temperature with increasing pressure is consistent with itinerant π^* electrons.

We dedicate this paper to J. M. Honig who has contributed much to the narrow-band problem in transition-metal oxides.

ACKNOWLEDGMENTS

The authors thank Dr. R. I. Dass for assistance with initial dc susceptibility measurements. The Robert A. Welch Foundation, Houston, Texas, is thanked for financial support.

REFERENCES

1. J. E. Greedan, *J. Less-Common Metals* **111**, 335 (1985).
2. D. A. MacLean, H.-K. Ng, and J. E. Greedan, *J. Solid State Chem.* **30**, 35 (1979).
3. C. W. Turner and J. E. Greedan, *J. Solid State Chem.* **34**, 207 (1980).
4. J. P. Goral, J. E. Greedan, and D. A. MacLean, *J. Solid State Chem.* **43**, 244 (1982).
5. Y. Okimoto, T. Katsufuji, Y. Okada, T. Arima, and Y. Tokura, *Phys. Rev. B* **51**(15), 9581 (1995).
6. K. Yoshii and A. Nakamura, *J. Solid State Chem.* **133**, 584 (1997).
7. K. Yoshii and A. Nakamura, *J. Solid State Chem.* **137**, 181 (1998).
8. G. Amow, J. E. Greedan, and C. Ritter, *J. Solid State Chem.* **141**, 262 (1998).
9. J. B. Goodenough, *Prog. Solid State Chem.* **5**, 145 (1971).
10. Y. Okada, T. Arima, Y. Tokura, C. Muruyama, and N. Mori, *Phys. Rev. B* **48**(13), 9677 (1993).
11. G. Amow and J. E. Greedan, *J. Solid State Chem.* **141**(1), 262 (1996).
12. J. B. Goodenough, "Magnetism and the Chemical Bond," Interscience and Wiley, New York, 1961.
13. A. H. Cooke, N. J. England, N. F. Preston, S. J. Swithenby, and M. R. Welts, *Solid State Commun.* **18**, 545 (1976).
14. C. W. Turner and J. E. Greedan, *J. Magn. Magn. Mater.* **20**, 165 (1980).
15. C. W. Turner, M. F. Collins, and J. E. Greedan, *J. Magn. Magn. Mater.* **23**, 265 (1981).